AMSER Rad Path Case of the Month:

A Side-By-Side Case Study of Neuroblastic Tumors

Colin M. Johnson, M.D., Tristan R. Young, M.D.
Medical University of South Carolina
Jeanne G. Hill, M.D.
Department of Radiology
Laura S. Spruill, M.D., Ph.D.
Department of Pathology
Laura Hollinger, M.D.
Department of Surgery
Medical University of South Carolina

MUSC
Medical University of South Carolina

AMSER

Patient Presentation

Patient A

HPI:

- 3 y.o. female presenting with a two-week history of constipation and new-onset urinary retention.
- The patient demonstrates clear discomfort when attempting to void and is passing small, hard stool despite OTC miralax and suppositories.
- The patient's mother denies observing any blood in the urine or stool.
- No fever, fatigue, or change in PO intake.

Physical Exam Findings:

- Mild abdominal distension without any palpable masses.
- Mild discomfort with suprapubic pressure.

Patient B

HPI:

- 4 m.o. male originally seen at 6 weeks for a follow-up of a sacral dimple noted at birth.
- Born at 40 weeks via C section, developing appropriately.
- Infant was asymptomatic with no complaints from parents.

Physical Exam Findings:

- No abnormal physical exam findings besides the sacral dimple, previously seen at birth.

What is the appropriate imaging work-up for each of these patients?

In a pediatric patient with constipation and urinary retention, concern for possible intra-abdominal pathology should first be evaluated with an abdominal radiograph. Any abnormal findings on initial imaging may determine the need for follow-up cross-sectional imaging.

While not uncommon in newborns, a sacral dimple is the most common cutaneous manifestation of dorsal malformations of the embryo (occult spinal dysraphism (OSD)), appearing in 12.8% of patients with OSD in a recent study. Because of this, Ultrasound or MRI are often used to evaluate for underlying pathology. Ultrasound is typically the initial examination as it is readily available, less expensive, and does not require sedation.

Initial Imaging

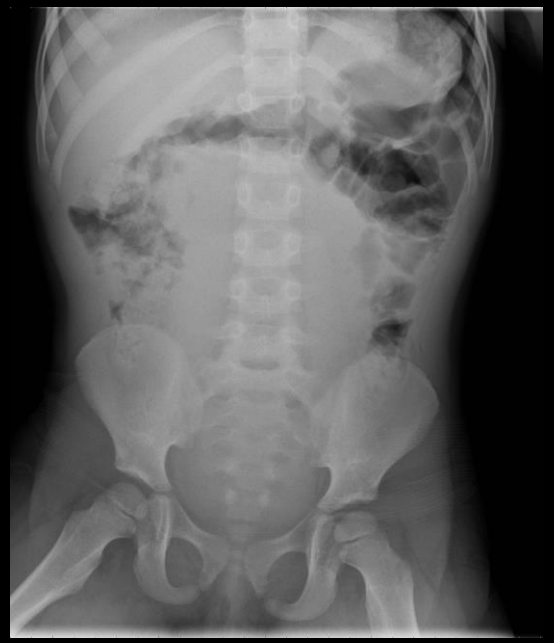

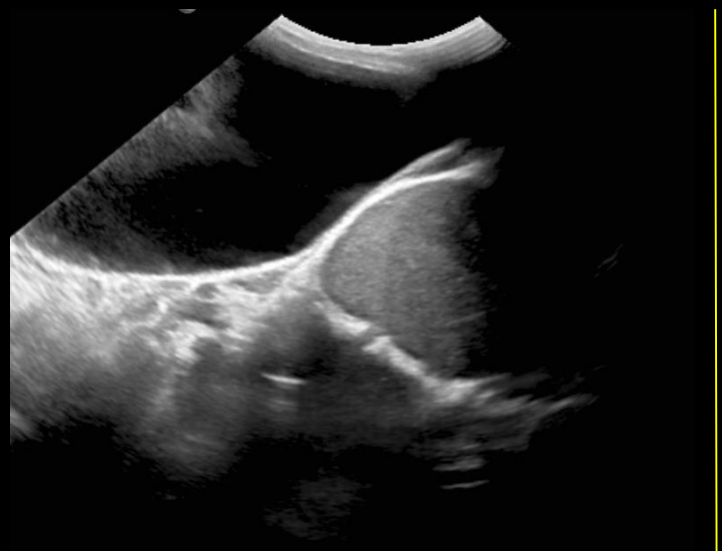

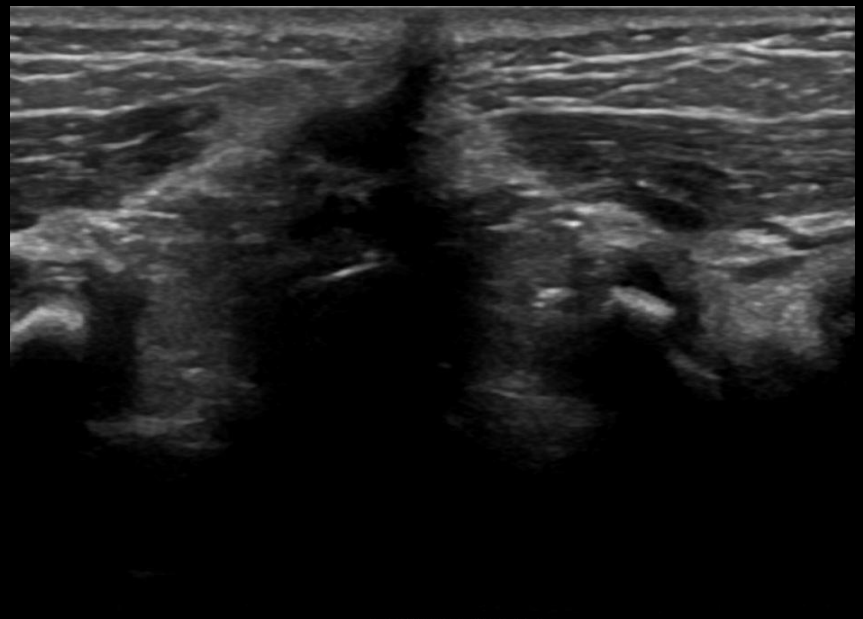

Initial Imaging

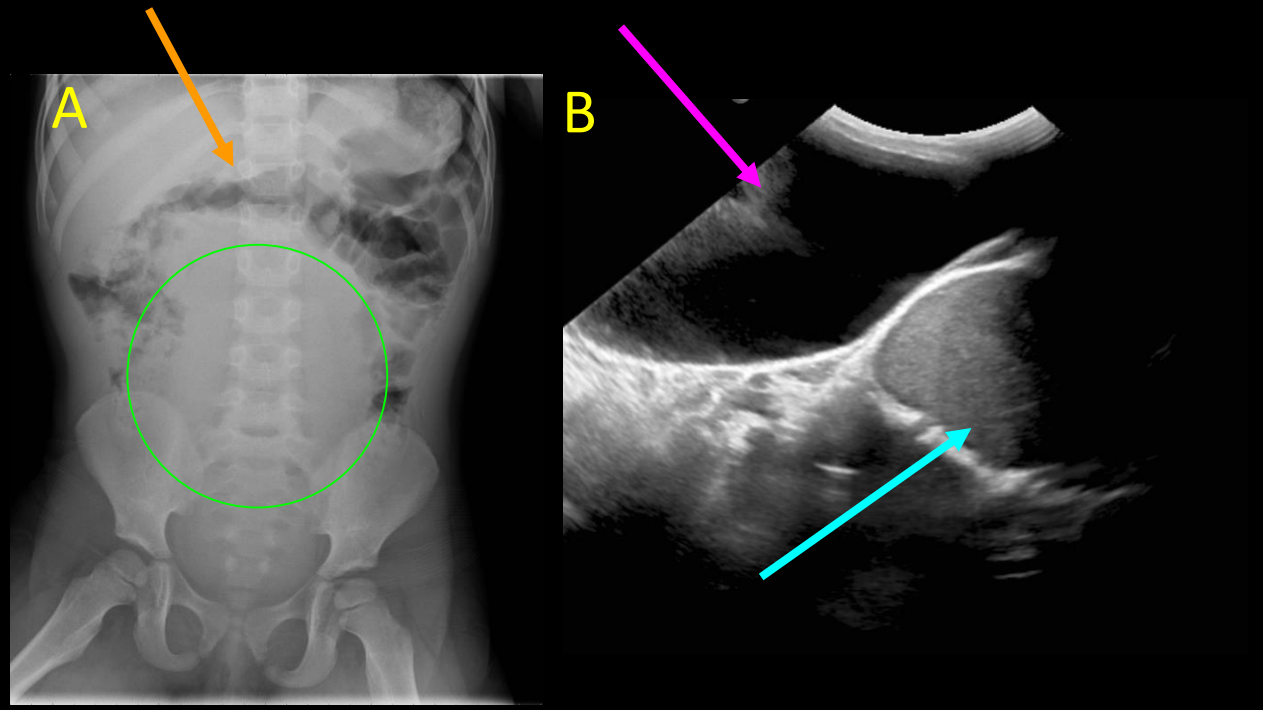

Abdominal radiograph (A) demonstrating a non-obstructive bowel gas pattern and moderate stool burden. The transverse colon has been displaced superiorly (orange arrow) and there is a suspicious paucity of bowel gas in the central abdomen (green circle).

Ultrasound (sagittal view, B) reveals a distended bladder (purple arrow), abutted by a partially-visualized hyperechoic presacral mass (blue arrow).

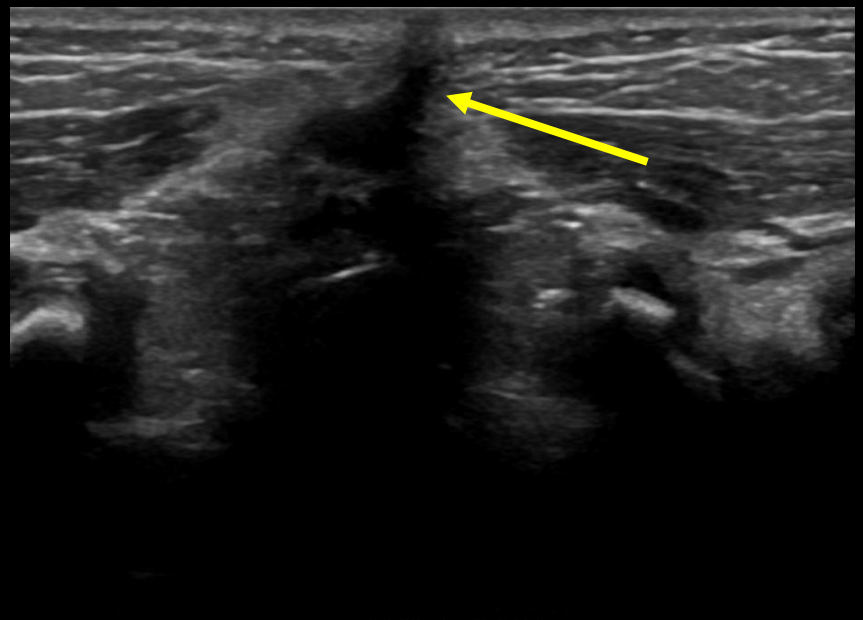

Transverse US of the spine underlying the sacral dimple. There is evidence of a connection between the sacral dimple and the spinal canal by means of a dermal sinus tract (yellow arrow).

Follow-up imaging with MRI is warranted in this patient to further evaluate the dimple and tract.

Follow-up Imaging

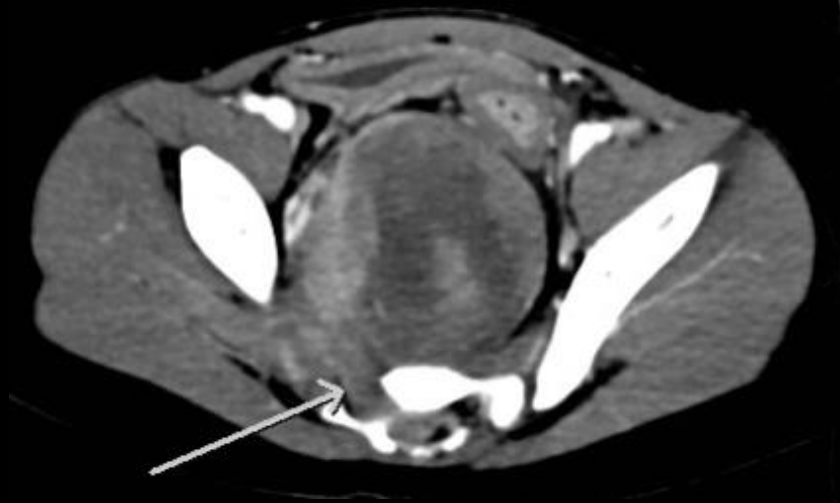

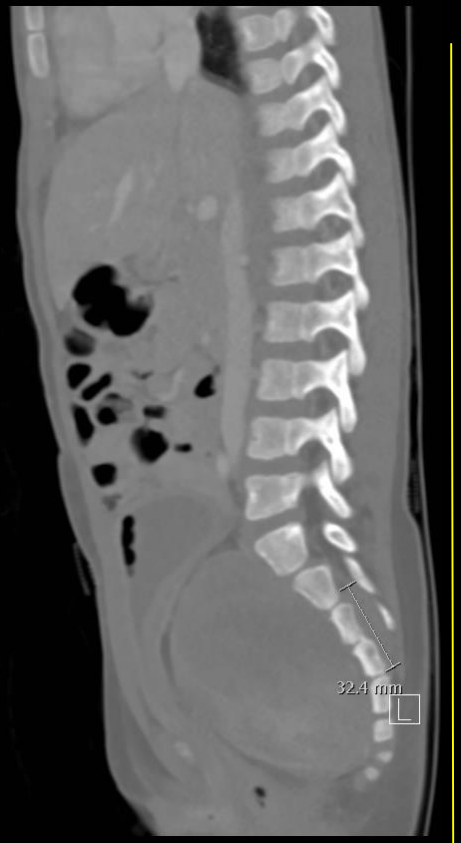

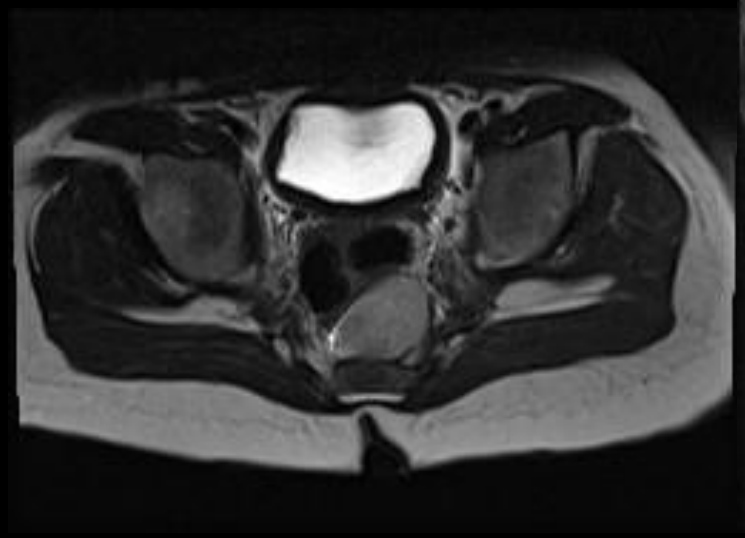

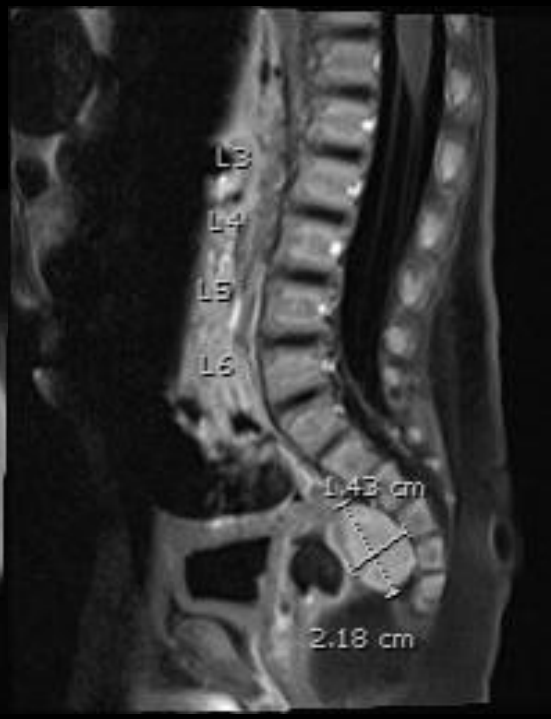

Follow-up Imaging

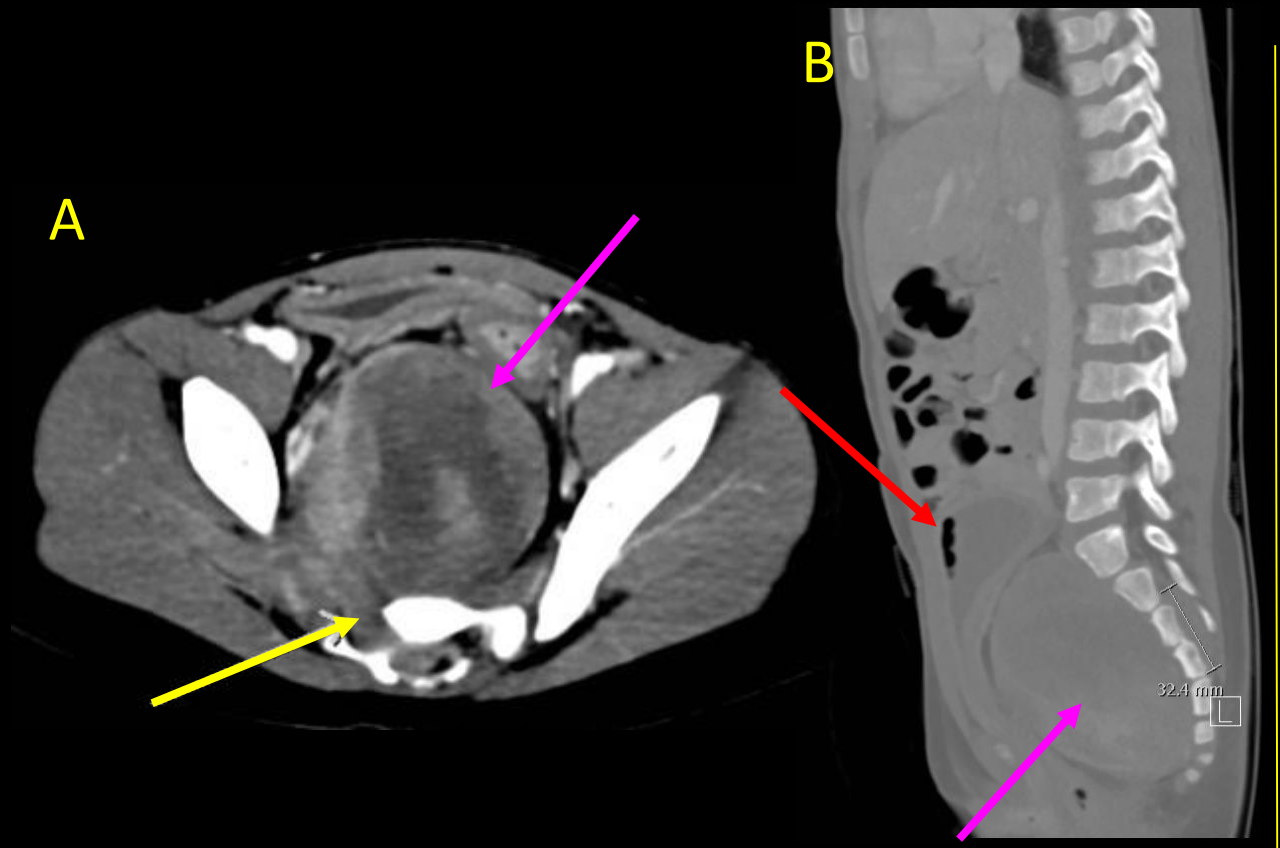

Axial CT Abdomen/Pelvis w/ contrast (A) demonstrating a heterogeneously enhancing, solid presacral mass, measuring 8.6. x 7.0 x 6.5 cm (purple arrows). The mass clearly invades the spinal canal via the sacral foramina (yellow arrow). The sagittal view (B) demonstrates the 3.2 cm extension of the mass into the spinal canal. Additionally, the bladder contains some free air secondary to decompressive foley catheterization (red arrow).

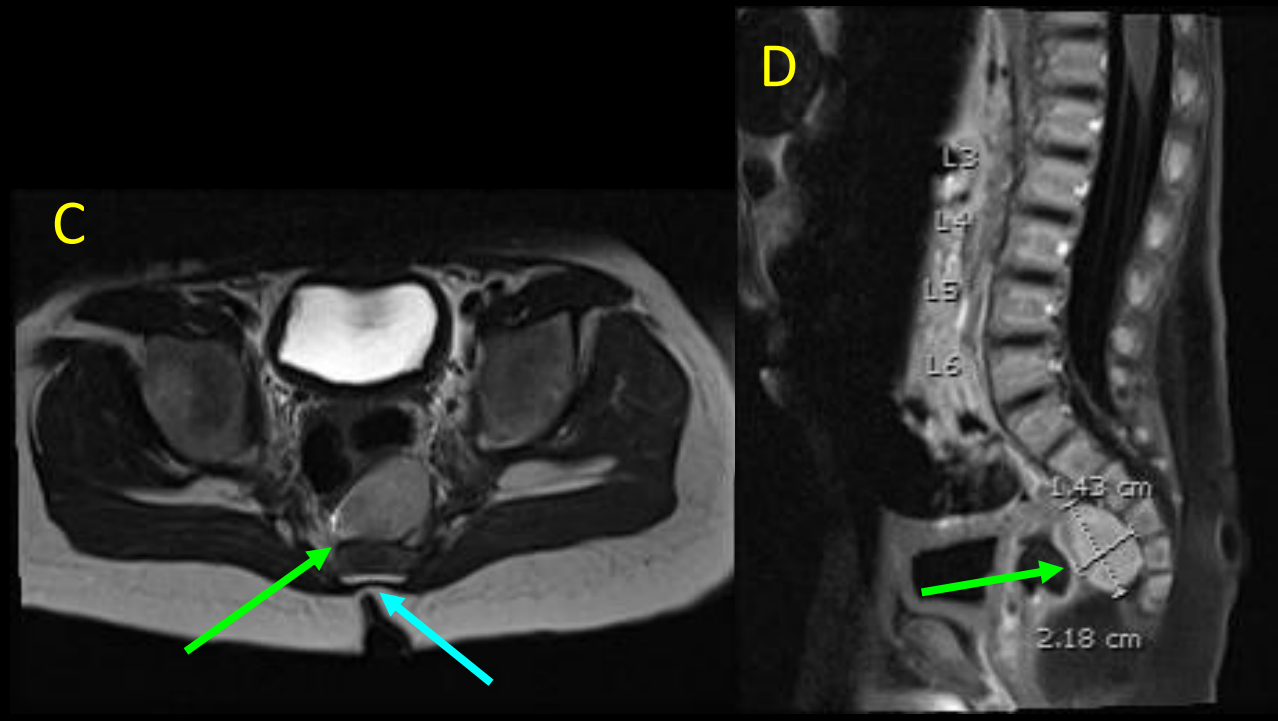

Axial T2 MRI (C) and sagittal T1 FLAIR (D) views demonstrate a homogenous, fairly well-circumscribed 2.2 cm x 1.4 cm presacral mass (green arrows) with suggestion of extension towards (but not into) the left lower sacral neural foramen. There is no epidural extension of the mass. There is a fibrous band that extends from the sacral dimple to the coccyx (blue arrow) with no connection to the thecal sac.

AMSER

DDX

- Neuroblastoma
- Ganglioneuroblastoma
- Ganglioneuroma
- Sacrococcygeal Teratoma
- Lipoma
- Dermoid Cyst
- Anterior Sacral Meningocele

Intraoperative Images

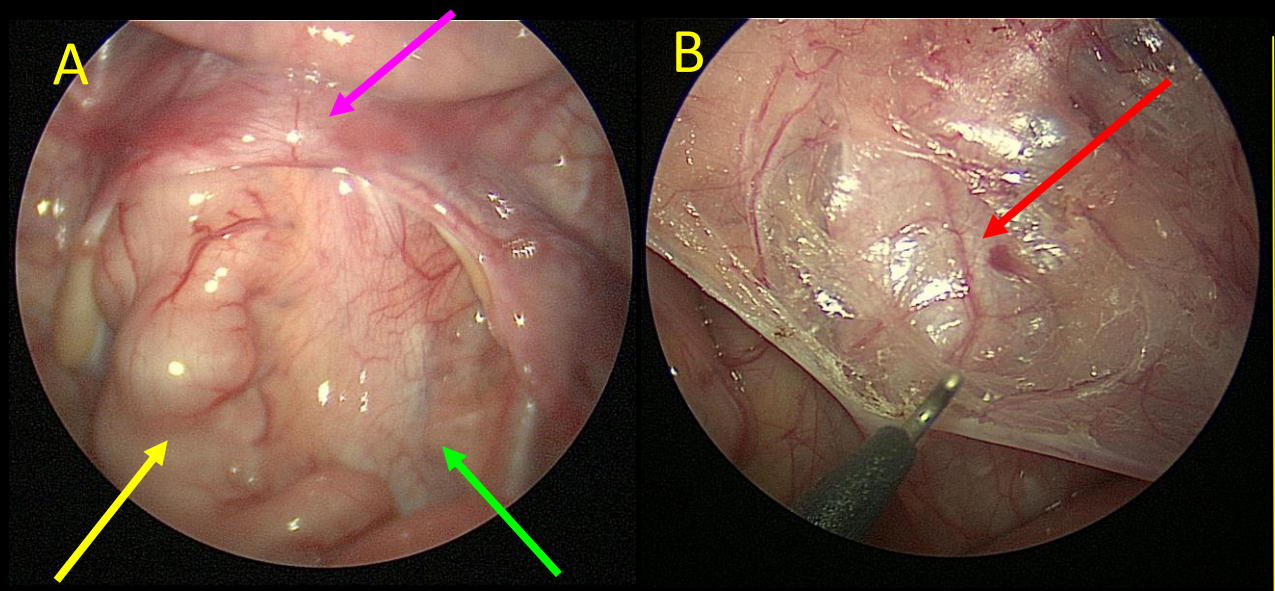

Intraoperative images of presacral mass debulking procedure. In the first image (A), the anatomy is clearly distorted by the underlying mass-effect of the presacral lesion. The rectum is displaced laterally (yellow arrow) and the pelvic veins are dilated (green arrow). The uterus is also displaced anteriorly by the mass (purple arrow).

In the second image (B), the mass can be seen after initial peritoneal dissection (red arrow). The rectum is up and out of view in this image.

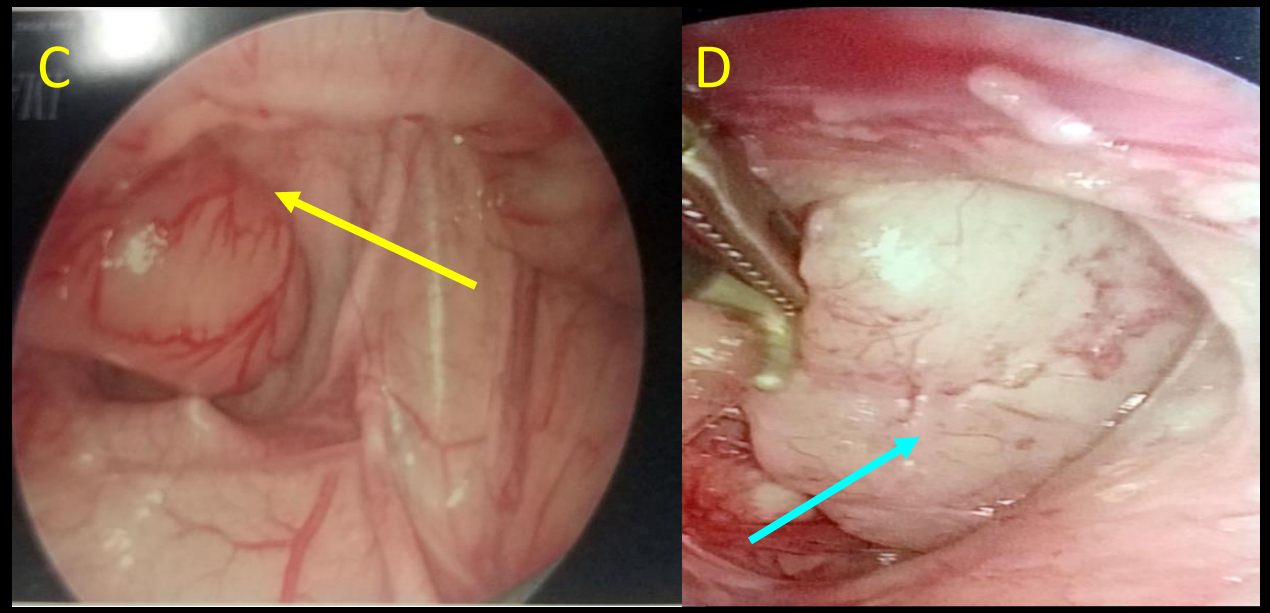

Intraoperative images of presacral mass resection. Image C is similar to image A, but there is no displacement of the rectum (yellow arrow) as the mass was considerably smaller in this patient. In image C, a portion of the rectum is held out of view by a surgical tool.

Image D demonstrates a clear view of the mass (blue arrow) after the peritoneum has been dissected away.

AMSER

Pathology (Micro)

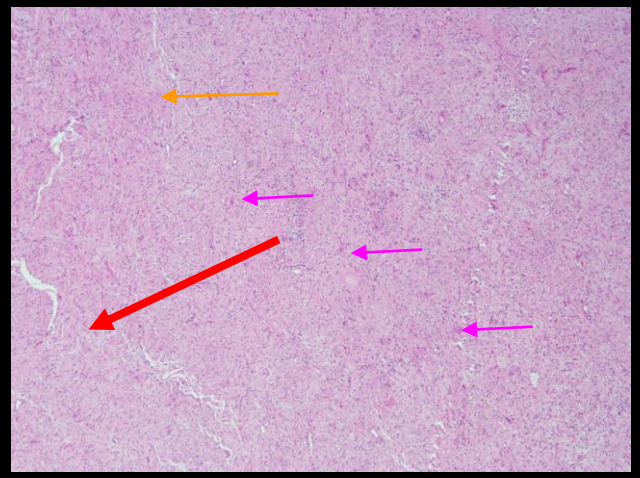

On low power H&E, there is a uniform sheet of eosinophilic, fibrillar stroma. The majority of the stroma is organizing into fascicles (red arrow) and palisading verocay-like structures (orange arrow). There are numerous well-differentiated ganglion cells throughout the stroma (purple arrows).

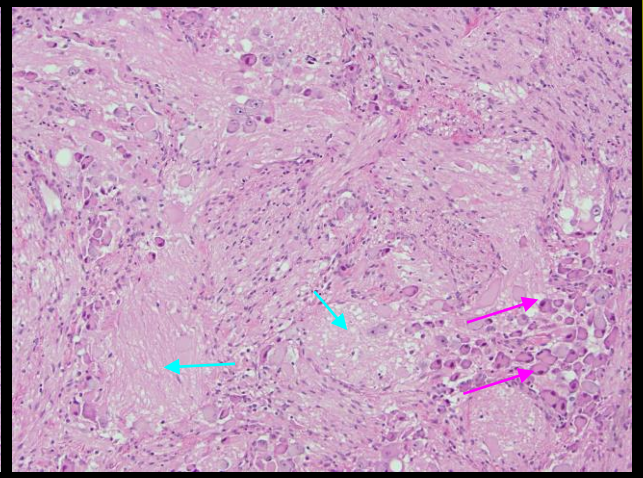

On higher power, there are pools of bubbly, amorphous neuropil, intermixed with the more structured, “Schwannian” elements of the stroma (blue arrows).

This neuropil represents the immature component of the histology.

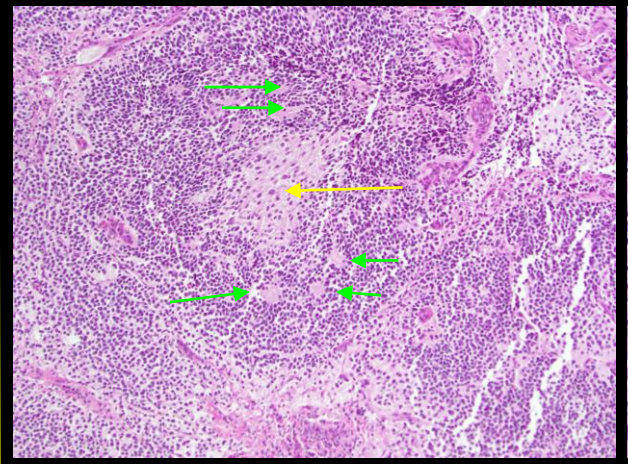

On low power H&E, there are numerous small, round blue cells. There is also some neuropil present (yellow arrow), surrounded by cells demonstrating rosettes (green arrows).

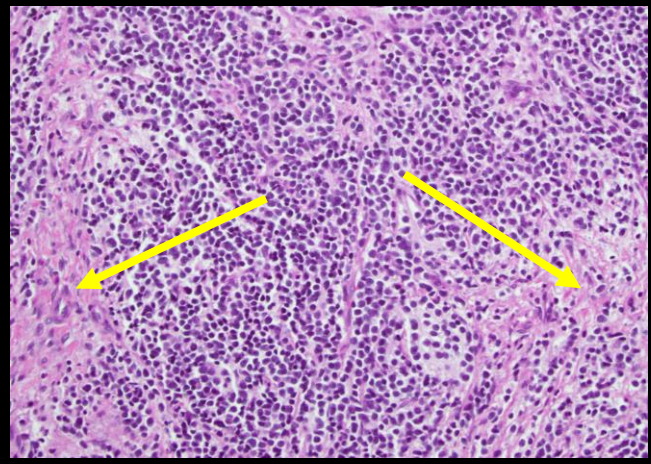

On higher power, there are multiple iconic small round blue cells in addition to the presence of neuropil (yellow arrows), both important for the histological classification of these tumors.

AMSER

Final Dx

Patient A: Ganglioneuroblastoma

Patient B: Neuroblastoma

Post-Resection Imaging (Patient B)

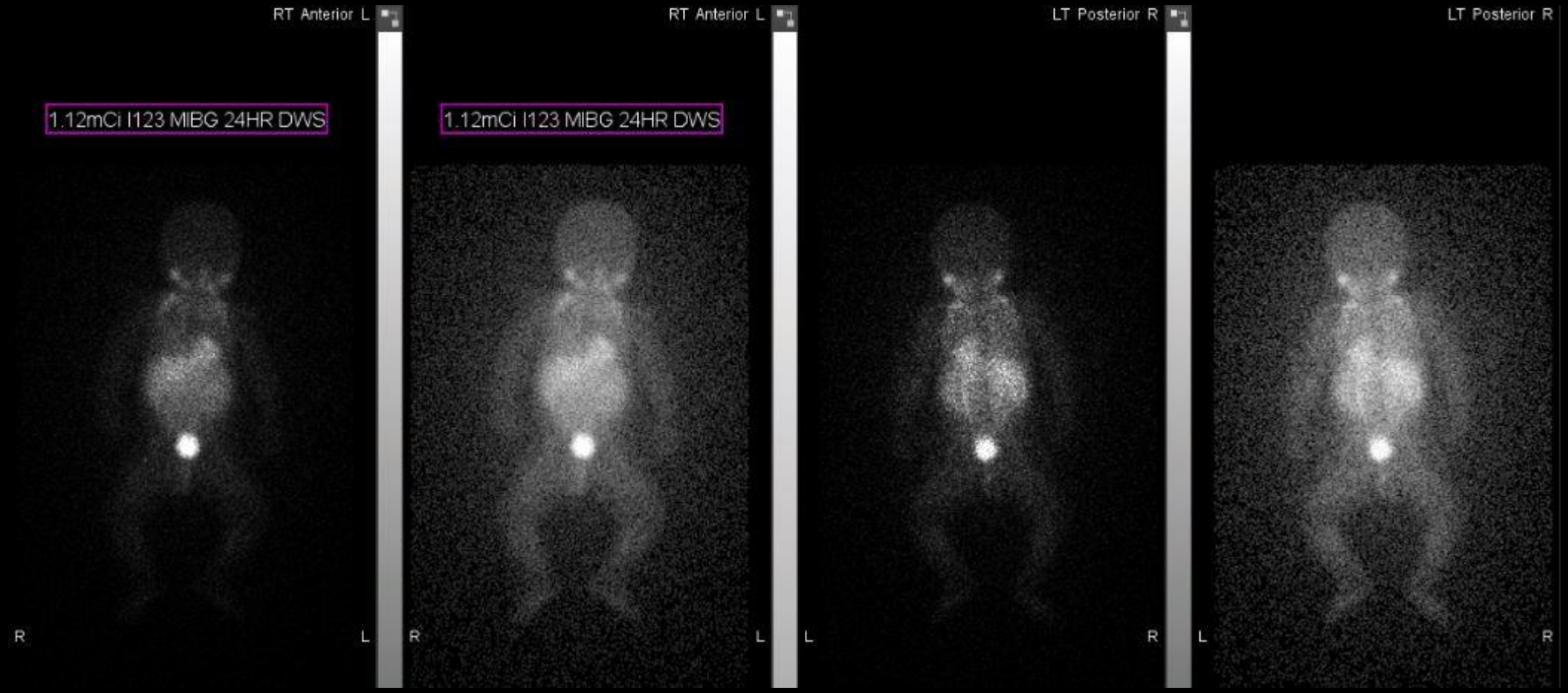

Post-resection 24 hr Whole Body planar images from an MIBG scan demonstrating no evidence of metastatic or residual disease. Physiologic activity is present within the salivary glands, oropharynx, liver, heart, regions of brown fat (shoulders), and urinary bladder. Curie Score = 0.

Discussion (Neuroblastic Tumors)

- Neuroblastic tumors are neoplasms of the sympathetic nervous system and therefore can arise wherever sympathetic tissue exists, e.g. neck, posterior mediastinum, pelvis, and abdomen. The most common location for these tumors is within the adrenal medulla. In the case of the two patients detailed in this report, the presacral nervous tissue was the point of tumor nucleation (though this is quite uncommon). These tumors are most commonly observed in patients < 10 y.o.

- Three subtypes of neuroblastic tumors exist. In increasing order of tissue immaturity and tumor malignancy/aggression: ganglioneuroma, ganglioneuroblastoma, and neuroblastoma. The more aggressive/immature tumors tend to occur in younger patients (median age: 2 y.o.), while the more benign/mature tumors tend to occur in older patients (median age: 7 y.o.).

- Neuroblastic tumors have a wide range of biologic activity, even in the more histologically aggressive varieties (neuroblastoma). Many prognostic factors have been linked to their malignant potential, including histological characteristics, proto-oncogene expression, DNA content, and catecholamine biosynthesis.

- The clinical presentation for neuroblastic tumors is incredibly variable, but abdominal distension and pain (from local mass-effect) are the most common presenting symptoms. Neurologic symptoms may also be present depending upon the location of the tumor (e.g. Horner's syndrome for paraganglionic tumors of the cervical chain).

Discussion (Neuroblastic Tumors)

- Diagnosis of neuroblastic tumors is made with a combination of imaging and histologic analysis. These tumors are most commonly discovered incidentally on physical examination and worked up with U/S or abdominal XR. Contrast-enhanced computed tomography is frequently the most useful staging imaging study to evaluate a suspected neuroblastic tumor after it has been discovered on initial imaging studies.

- Ancillary tests useful for the analysis of neuroblastic tumors include the measurement of catecholamine metabolites (e.g. vanillylmandelic acid [VMA] and homovanillic acid [HVA]), quantification of proto-oncogene expression (e.g. N-MYC), and evaluation for a loss of heterozygosity on the short (p) arm of chromosome 1.

- Management of neuroblastic tumors is largely defined by the International Neuroblastoma Staging System (INSS), which stages these tumors based on clinical, radiologic, and surgical characteristics. The INSS stage, paired with the results from the aforementioned ancillary analyses, ultimately guides management.

- Treatment most often includes a component of surgical debulking/resection augmented with varying degrees of chemotherapy.

Discussion (Neuroblastomas)

- Neuroblastomas are the most malignant variant of the neuroblastic tumors. Neuroblastomas can be found anywhere that sympathetic nervous tissue is located, along the sympathetic chain from the skull base to the pelvis. Most commonly, however, they arise within the adrenal glands (46%). An additional 18% of neuroblastomas are intra-abdominal, but extra-adrenal. 14% arise within the posterior mediastinum and thorax. Neuroblastomas are responsible for 10% of pediatric cancers and 15% of cancer deaths in this population. There is also a racial/ethnic predominance for these tumors in African Americans and Native Americans.

- Metastatic disease is found in 40-60% of patients upon presentation, with bone being the most common site.

- Histologically, this is a small round blue cell tumor. The round blue cells are immature neuroblasts, and when they are the vast majority of the visualized cells, such as in the case of Patient B, it favors a diagnosis of Neuroblastoma over the other two variants of neuroblastic tumors. The presence of neuropil and Homer-Wright rosettes (differentiated tumor cells surrounding neuropil) may also be visualized in Neuroblastomas.

- The Shimada Classification system and the International Neuroblastoma Pathology Classification (INPC) system are used to classify these tumors and predict prognosis. There are three subtypes in the INPC: undifferentiated, poorly differentiated, and differentiating. The amount of neuropil (lower the better) and percentage of differentiating neuroblasts (higher the better) are the main differentiating criteria for the subtypes.

Discussion (Neuroblastomas)

- Neuroblastomas have a variety of clinical manifestations, ranging from small tumors that spontaneously regress to large tumors that cause significant mass effect and metastatic disease. Genetic susceptibilities are believed to play a large role in the ultimate clinical course.

- Though Patient B's tumor was found incidentally, the clinical presentation often depends on tumor location and extension. If the tumor is large enough, adrenal and abdominal tumors can be palpated on physical exam. Some intra-abdominal tumors can cause hypertension from compression of the renal vessels. Thoracic and posterior mediastinal tumors can cause scoliosis or airway compression. Occasionally, posterior mediastinal masses are misdiagnosed as pneumonia on radiographs. Tumors invading the spinal canal may present with motor or sensory nerve deficits.

Discussion (Neuroblastomas)

- Neuroblastomas have distinct imaging characteristics. They tend to demonstrate areas of necrosis and dystrophic calcification. Calcifications are noted on plain XR in 30% of cases and on CT in 80-90% of cases. Other imaging characteristics include increased internal vascularity (on U/S), propensity to cross anatomical midline (classically posterior to the aorta), encasement of vascular structures, displacement of solid organs, and invasion of neural foramina/spinal canal.

- As an analog of norepinephrine, Iodine-123 metaiodobenzylguanidine (MIBG) is a functional imaging agent useful in identifying both the primary tumor and its associated metastases as it is taken up by 90% of neuroblastomas. The MIBG scan can also be used to predict the overall prognosis. The Curie Score, a semiquantitative scoring system developed to classify patients based on the extent of their MIBG uptake, is calculated by analyzing 10 anatomic segments (9 skeletal and 1 soft tissue). Each segment is scored 0-3 based on the number and extent of the lesions. The scores are summated and stratified. The major shortcoming of MIBG is that is is unable to distinguish between neuroblastomas and other tumors arising from sympathetic tissue (e.g. pheochromocytomas).

Discussion (Neuroblastomas)

- Neuroblastomas can also be associated with certain paraneoplastic syndromes. Two classic neuroblastoma-associated paraneoplastic syndromes are opsoclonus-myoclonus syndrome and increased secretion of vasoactive intestinal peptide (VIP). Opsoclonus-myoclonus syndrome is due to the patient's own antibodies attacking central nervous system antigens, leading to sporadic movement of the eyes and limbs ("dancing eyes, dancing feet"). Increased VIP secretion leads to profuse diarrhea and electrolyte imbalances. Removal of the tumor often leads to the resolution of the symptoms associated with increased VIP secretion. However, the immune response seen in opsoclonus-myoclonus syndrome may persist despite tumor resection.

- Prognosis can be highly variable, with both genetic factors and pattern of tumor spread affecting the outcome. An unusual type of neuroblastoma is the 4S pattern of metastatic spread. The 4S subtype typically consists of a small tumor found in children <1 year old, classically spreading to the skin ("blueberry muffin spots") and liver, which often regresses spontaneously without treatment. Children with the 4S subtype of neuroblastoma have a much better prognosis than patients age 12-18 months with metastases to the bone and bone marrow at diagnosis as the tumor often regresses spontaneously without treatment.

References

1. Lonergan, G. J., Schwab, C. M., Suarez, E. S., Carlson, C. L. Neuroblastoma, ganglioneuroblastoma, and ganglioneuroma: radiologic-pathologic correlation. *Radiographics,* 2002. *22*(4), 911-34.
2. Schwab, M., Westermann, F., Hero, B., & Berthold, F. Neuroblastoma: Biology and molecular and chromosomal pathology. *The Lancet Oncology,* (2003). *4*(8), 472-480.
3. Haveri, F. T., Inamadar, A. C. A cross-sectional prospective study of cutaneous lesions in newborn. *ISRN Dermatology*. (2014).
4. Brisse, H. J., Mccarville, M. B., Granata, C., Krug, K. B., Wootton-Gorges, S. L., Kanegawa, K., Monclair, T. Guidelines for Imaging and Staging of Neuroblastic Tumors: Consensus Report from the International Neuroblastoma Risk Group Project. *Radiology,* (2011). *261*(1), 243-257.
5. Lonergan, G. J., Schwab, C. M., Suarez, E. S., & Carlson, C. L. From the Archives of the AFIP. *RadioGraphics,* (2002). *22*(4), 911-934.
6. Bradeur, G. M., Bagatell, R. Mechanisms of neuroblastoma regression. *Nature Review Clinical Oncology*. (2014). 11, 704-713
7. Swift, C. C., Eklund, M. J., Kraveka, J. M., Alazraki, A. L. Updates in Diagnosis, Management, and Treatment of Neuroblastoma. *Radiographics*. (2018).

AMSER